

Phototransformation of riverine dissolved organic matter (DOM) in the presence of abundant iron: Effect on DOM bioavailability

Edith Kaiser¹ and Barbara Sulzberger

Swiss Federal Institute for Environmental Science and Technology, Ueberlandstrasse 133, CH-8600 Duebendorf, Switzerland

Abstract

We conducted studies with high-molecular-weight (HMW) and low-molecular-weight (LMW), hydrophobic, and hydrophilic dissolved organic matter (DOM) from an oligotrophic alpine river, the Tagliamento River (Italy), to assess the effect of light on DOM utilization by riverine bacterioplankton. Immediately after the exposure of the DOM fractions to simulated or natural sunlight, short-term (1 h) bacterial utilization of all DOM fractions decreased by up to 80%, compared with the uptake of the corresponding nonirradiated fractions. The addition of scavengers suggests that reactive oxygen species caused this bacterial growth inhibition. After the long-term growth of bacteria on irradiated DOM, uptake was unchanged for HMW DOM, considerably lower for LMW and hydrophilic DOM, and much higher for hydrophobic DOM, compared with the nonirradiated fractions. These results suggest that the phototransformation of HMW, LMW, hydrophobic, and hydrophilic DOM results in contrasting effects on their bioavailability. Size-exclusion chromatography showed that bacteria preferably used the larger molecular sizes of all nonirradiated fractions. Light induced no significant shifts in the apparent molecular weight distribution of the four DOM fractions. However, the highly bioavailable LMW DOM (especially the portion ~5 kDa) was no longer taken up after irradiation. We conclude that light overall leads to a strong decrease in microbial DOM transformation during hydrological transport in the Tagliamento River.

DOM represents a major reactive reservoir of organic carbon on Earth (Schlesinger and Melack 1981) and an essential energy resource for all microbial processes (Wetzel 1992). River systems are fundamental to global carbon cycling because they receive, produce, transport, and transform organic material and therefore integrate terrestrial and marine environments (Meybeck 1981; Hedges et al. 1997; Raymond and Bauer 2001).

In the past two decades, the importance of photochemical transformations on the cycling of organic carbon in aquatic systems has been recognized and intensively studied (Kieber et al. 1989; Benner and Biddanda 1998). Some of these studies have described the net effect of solar radiation on bacteria–dissolved organic matter (DOM) interactions. They showed that the photocleavage and photooxidation of high-molecular-weight (HMW) DOM led to a release of readily bioavailable low-molecular-weight (LMW) compounds that indirectly stimulated bacterioplankton activity and thus enhanced the turnover of DOM (Kieber et al. 1989; Wetzel et al. 1995). Other work proved that light leads to contrasting

effects on DOM, transforming bioavailable into biorecalcitrant compounds and vice versa (Benner and Biddanda 1998; Obernosterer et al. 1999). In surface marine waters and humic lakes, sunlight has also been found to abiotically remineralize a large portion of DOM to carbon monoxide/carbon dioxide and inorganic nutrients such as phosphate and ammonium (Cotner and Heath 1990; Bushaw et al. 1996; Johannssen and Miller 2000). Some studies have characterized light-induced changes in DOM bulk chemical composition using ¹³C nuclear magnetic resonance (NMR) spectroscopy (Wetzel et al. 1995; Clair and Sayer 1997). Opsahl and Benner (1998) investigated light-induced changes in the dissolved lignin composition, with lignin being an important biomarker for terrestrial organic biomass transported by rivers to the marine environment. Although the literature provides ample information on DOM phototransformations in lake and surface ocean environments, we lack knowledge on the effect of sunlight on riverine carbon cycling (Amon and Benner 1996).

Rivers carry high amounts of particulate and colloidal iron that they receive through the weathering of minerals (e.g., biotite) in the catchment area and the oxidative precipitation of Fe(II). In iron-rich surface waters, light-induced redox cycling of iron and DOM photo-oxidation are strongly coupled. Iron can catalyze DOM photo-oxidation via ligand-to-metal charge transfer reactions of Fe(III)-DOM complexes and through DOM oxidation by the hydroxyl radical (HO•) formed in the Fenton reaction (Miles and Brezonik, 1981; Voelker et al. 1997). The direct photooxidation of DOM (i.e., electron transfer from triplet-excited functional groups of DOM to ground-state molecular oxygen) yields superoxide (O₂^{•-}), which reacts to H₂O₂ by (iron-catalyzed) dismutation (Blough and Zepp 1995; Voelker et al. 1997). In addition, oxidation of Fe(II) by oxygen and subsequent reactions also produce transient species O₂^{•-}, H₂O₂, and HO• (e.g., Moffet

¹ Present address: Swiss Federal Institute of Environmental Science and Technology, Seestrasse 79, CH-6047 Kastanienbaum, Switzerland (edith.kaiser@eawag.ch).

Acknowledgments

We are grateful to the Tagliamento Research Group for enormous help with water sampling and other field work. We especially thank Hans-Ulrich Laubscher and Sebastian Hesse for help with sample measurements and Ronald Benner for his enthusiasm and constant advice to make this work possible. Many critical comments by Laura Sigg, Silvio Canonica, and Stephan Hug helped improve the manuscript considerably. We also thank Christopher Robinson for language editing.

This work was supported by the Swiss Federal Institute for Environmental Science and Technology.

and Zika 1987; Emmenegger et al. 1998). Major sinks of O_2^- are oxidation and reduction of iron and copper species, and reaction with DOM (Goldstone and Voelker 2000). In addition to H_2O_2 , long-living organic peroxides also are produced in photochemical and subsequent thermal reactions of DOM (von Sonntag and Schuchmann 1997).

Reactive oxygen species (ROS), such as $O_2^{\bullet-}$, H_2O_2 , and HO^{\bullet} , organic peroxy radicals (RO_2^{\bullet}), and organic peroxides, resulting from photochemical and subsequent thermal reactions of DOM and iron, have been shown to severely damage the cell structure and physiology of aquatic microorganisms (Fridovich 1986). For example, reactive species initiate the oxidation of chlorophyll and the peroxidation of lipids and inhibit carbon fixation and the motility of dinoflagellates. However, we still know little about their effect on bacterial activity. As a defense against active forms of oxygen, microorganisms have developed various biochemical antioxidants, quenchers, and scavengers (Chow 1988), such as tocopherols, carotinoids, ascorbate, urate, and enzymes.

In the Tagliamento River, light may significantly penetrate the water column because of low turbidity and shallow depth of the water bodies and be absorbed by DOM or iron-DOM complexes. Therefore, one important question is how well cells can use DOM that has been exposed to sunlight in this alpine river system. To increase our understanding of the overall effect of light on bacterial DOM utilization, we studied different fractions of DOM. Over >1 yr, we collected water bimonthly in a longitudinal and lateral direction from the Tagliamento River (Fig. 1). We size and chemically fractionated these water samples to collect HMW, LMW, hydrophobic, and hydrophilic DOM. These four fractions were used for photochemical and bioassay experiments. The purpose of our research was to determine the short- and long-term effects of the irradiation of DOM fractions on their utilization by natural bacterioplankton and to relate light-induced changes in the bioavailability of DOM fractions to changes in their chemical composition.

Materials and methods

Study area and sample collection—The river corridor of the Tagliamento River has been extensively studied since 1997 (Ward et al. 1999; van der Nat 2002). The river is classified as the last large natural river in Europe (northeast Italy) (Ward et al. 1999), extending over 170 km and flowing unrestrained from the alpine headwater reaches to the northern Adriatic Sea (Fig. 1). Its highly complex channel morphology is characterized by constrained, braided, and meandering reaches formed by a dynamic hydrological regime. The Tagliamento River experiences two major flood periods each year (spring and fall), which facilitates the deposition and mobilization of materials and leads to major changes in organic matter input and transport.

Water samples for DOM fractionation were collected seasonally from the main channel (MC) in the island-braided headwater floodplain (R2), in the island-braided lower and major floodplain (R4), and in the braided-to-meandering transition floodplain (R5) and from one isolated pool in R4 (Fig. 1). Field sampling took place during March, May, July,

August, October, and November 1999 and April, July, and August 2000. During sampling, water levels varied from low- to high-flow conditions (Table 1). Over the year, water temperatures in the main channel were $10.9 \pm 2.5^\circ\text{C}$, pH 8.13 ± 0.14 , and alkalinities $2.8 \pm 0.5 \text{ mmol L}^{-1}$. Water samples (~200 liters per sampling station) for DOM fractionation were collected with clean 50 L high-density polyethylene carboys and transported to the field laboratory near the Tagliamento River at R4. Immediately after collection, water samples were passed through muffled GF/F filters and 0.2- μm Durapore filters (142 mm diameter; Millipore) and stored in clean 50-L carboys.

DOM fractionation—DOM was either chemically or size fractionated, except in April 2000, when both methods were used in parallel. For chemically fractionating DOM into hydrophobic- and hydrophilic-type compounds, a Mega Bond Elute C18 column (C18 loaded silica, 60CC; Varian) was used after acidification with 32% hydrochloric acid (Suprapur) to pH 2.8 (Louchouart et al. 2000). Before fractionation, the water was acidified. Flow rates ranged 3–5 L h^{-1} . Of the total DOC (DOC <0.2 μm), 13–54% was recovered as a sorbed hydrophobic fraction (Table 1), which is comparable to other values in the literature (Amador et al. 1990). A Filtron tangential flow ultrafiltration system with a polyethersulfone membrane (1 kDa nominal weight cutoff) was used for fractionating bulk DOM into pseudo HMW and LMW portions, according to the protocol of Benner et al. (1997). Operating pressures were 137.9–151.7 kPa at the inlet and 68.9–89.6 kPa at the outlet. Filtration rates ranged 6–8 L h^{-1} using one 0.46- m^2 cassette filter (Centrasette; Filtron). Water temperature ranged 20–22°C during ultrafiltration. Recovery was 8–29% of the total DOC (Table 1). For every sample, a carbon mass balance was established, to determine whether carbon was lost or gained during fractionation. Mass balance calculations revealed recoveries of 99–144% for ultrafiltration and 100–139% for C18 solid phase extraction. The percentage of DOC recovered after fractionation from bulk DOC was calculated as follows: % DOC retained = $100 \times (\text{DOC}_{\text{retentate}} + \text{DOC}_{\text{permeate}}) \times (\text{DOC}_{<0.2\mu\text{m}})^{-1}$, where DOC stands for DOC concentration and was corrected by the according concentration factor (CF) (Table 1). The CF was calculated as follows: CF = initial sample volume/retentate volume.

From fractionation, samples were stored at 4°C in the dark and immediately transported to the laboratory in Switzerland (Swiss Federal Institute for Environmental Science and Technology). DOM adsorbed onto the C18 phase was eluted by gentle vacuum filtration using high-purity methanol (Merck). The methanol was removed from DOM by rotoevaporation and freeze drying. Next, the extract was redissolved in MQ-UV water (Millipore). For further photochemical experiments, hydrophobic and HMW DOM were rediluted with MQ-UV water to reach final DOC concentrations of ~100 $\mu\text{mol L}^{-1}$ C, which was in the range of total organic carbon (TOC) concentrations measured from raw river water.

TOC and DOC measurements—Water samples (20 ml) were collected directly after fractionation for ultrafiltered

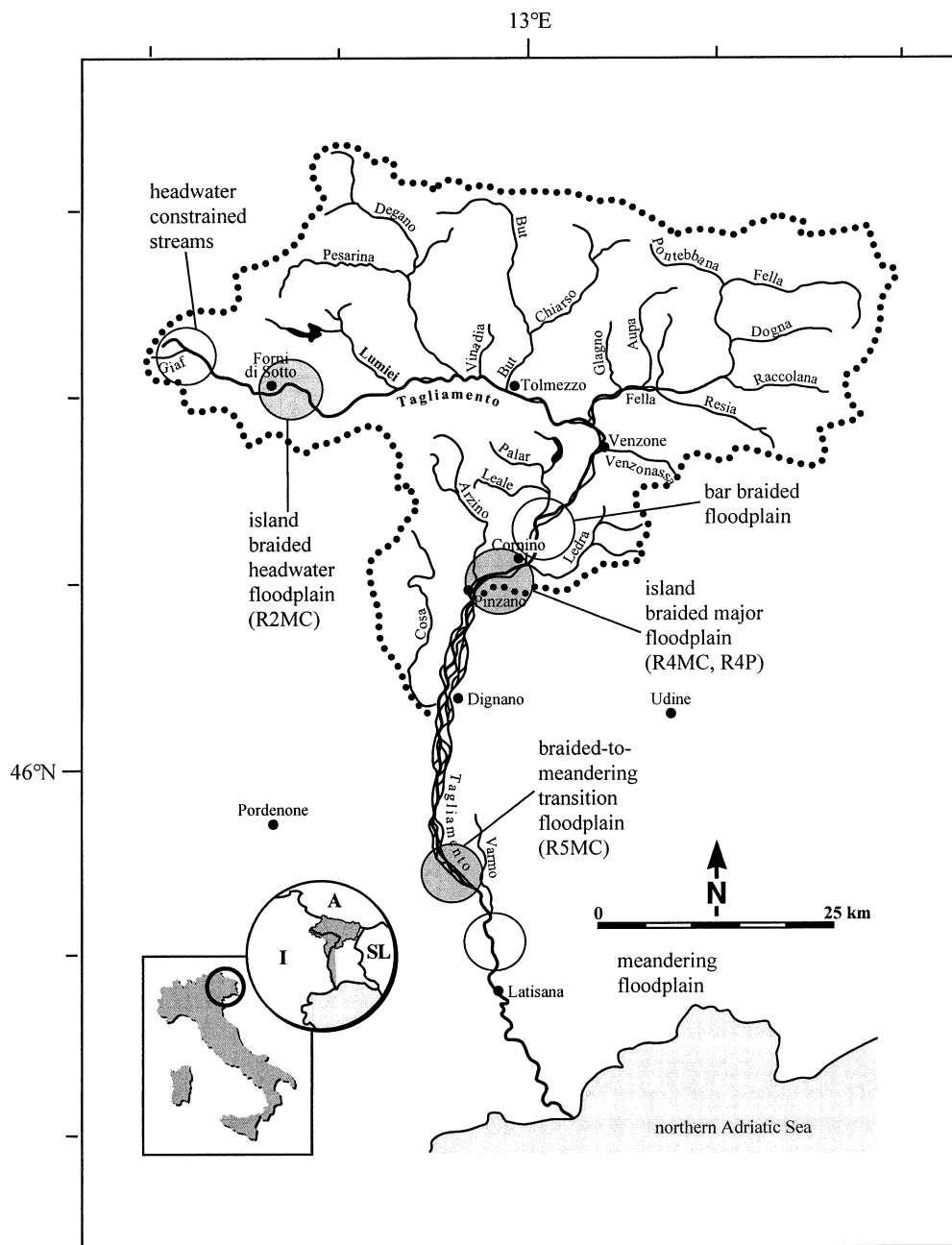


Fig. 1. Catchment of the Tagliamento River with sampling stations marked by gray circles: the main channel in the headwater floodplain (R2MC), in the major floodplain (R4MC), and in the transition floodplain (R5MC), and an isolated pool in the major floodplain (R4P). The small inset shows that the river is located in northeast Italy, Europe.

samples and after freeze-drying and redissolution in MQ-UV water for solid phase extracted DOM. The samples were filled in acid-rinsed, precombusted 40-ml EPA glass vials, sealed with Teflon-lined caps, and stored frozen until analysis. TOC and DOC concentrations were determined by high-temperature catalytic oxidation with a Shimadzu 5050A analyzer (Benner and Strom 1993; Benner et al. 1997).

Size exclusion chromatography (SEC)—Water samples for SEC were collected in muffled 10-ml ampoules or acid-

rinsed, muffled 40-ml EPA glass vials (Wheaton), sealed with Teflon-lined caps, and stored frozen until analysis. We used gel permeation chromatography (TSKHW50S) with UV absorbance (at 254 nm) and DOC detection to characterize the apparent molecular weight distribution of the DOM fractions before and after irradiation (Mueller et al. 2000). The detection of DOC was based on the absorption of infrared light by CO_2 from photo-oxidized DOC. The mobile phase was composed of “carbon-free” water (UV-photo-oxidized MQ-UV water; Millipore), 3.6 mmol L^{-1} sodium

Table 1. Sample descriptions, dissolved organic carbon (DOC) and dissolved iron (DI) concentrations in the individual DOM fractions, DI as % of bulk DI measured in bulk DOM ($<0.2 \mu\text{m}$), Fe(II) steady-state concentrations ($[\text{Fe(II)}]_{\text{ss}}$ as % of DI, and net H_2O_2 formation. Data represent averages (\pm SE) of seasonal samples ($n = 3\text{--}5$). DOC concentrations of HMW and hydrophobic DOM are corrected by the concentrator factor calculated from ultrafiltration and C18-solid phase extraction.

Sampling location, and DOM fraction	DOC ($\mu\text{mol L}^{-1}$)	DI (nmol L^{-1})	DI as % of bulk DI	$[\text{Fe(II)}]_{\text{ss}}$ ($\text{nmol L}^{-1}/1 \text{ mg C L}^{-1}$)	$[\text{Fe(II)}]_{\text{ss}}$ (% of DI)	Net H_2O_2 formation ($\text{nmol L}^{-1} \text{ h}^{-1}/(1 \text{ mg C L}^{-1})$)
R2MC						
Hydrophobic	17 ± 5	5.0 ± 3.0	30 ± 14	0.3	2	95
Hydrophilic	45 ± 7	10.5 ± 2.2	83 ± 31	7.1 ± 6.2	27 ± 24	257 ± 90
HMW	13 ± 3	2.6 ± 0.8	13 ± 1	3.4 ± 1.6	20 ± 11	6 ± 4
LMW	76 ± 3	22.2 ± 15.8	45 ± 10	0.6 ± 0.3	1	248 ± 9
R4MC						
Hydrophobic	19 ± 7	14.0 ± 6.0	44 ± 14	0.7 ± 0.6	2 ± 1	43
Hydrophilic	48 ± 8	35.9 ± 9.6	49 ± 20	1.2 ± 0.8	4 ± 2	282 ± 18
HMW	20 ± 4	12.8 ± 4.6	38 ± 14	2.1 ± 0.9	4 ± 3	83 ± 33
LMW	91 ± 14	13.3 ± 4.5	23 ± 2	0.3 ± 0.2	4 ± 2	201 ± 65
R4P						
Hydrophobic	18 ± 5	12.0 ± 11.0	84 ± 3	0.7 ± 0.4	3.1 ± 1	23
Hydrophilic	30 ± 3	15 ± 5	83 ± 57	4.9 ± 2.2	12 ± 6	431 ± 147
HMW	10 ± 3	10.6 ± 6.9	28 ± 10	3.2 ± 1.4	12 ± 7	88 ± 56
LMW	65 ± 14	9.6 ± 2.8	76 ± 64	0.5 ± 0.2	4 ± 2	293 ± 73
R5MC						
Hydrophobic	19 ± 8	6.0 ± 4.0	32 ± 9	nd	nd	63
Hydrophilic	31 ± 4	12.1 ± 3.4	59 ± 19	12.7 ± 10	24 ± 17	315 ± 102
HMW	12 ± 3	4.9 ± 1.1	40 ± 7	2.5 ± 0.6	6 ± 1	101 ± 50
LMW	64 ± 11	16.2 ± 9.4	104 ± 77	0.4 ± 0.3	2 ± 1	133 ± 9

MC: main channel, nd: not determined, P: isolated pool in major floodplain, R2: headwater floodplain, R4: major floodplain, R5: lower floodplain.

hydrogen phosphate, and 18.4 mmol L^{-1} potassium hydrogen phosphate (pH 6.6). Potassium hydrogen phosphate was also used for calibration. A variety of organic model substances were used to describe the size exclusion of different molecular weight ranges between 200 and 0.1 kDa (Huber and Frimmel 1992). Humic substances, LMW organic acids, polysaccharides, proteins, and amphiphilic and hydrophobic organic substances were used for qualitative interpretations of chromatograms obtained with the DOM fractions. We calculated the apparent molecular size distribution after Perminkova et al. (1998).

Total and dissolved iron ($[\text{Fe(II)}]$ and $[\text{Fe(III)}]$) measurements—Before and after DOM fractionation, all water samples were collected in clean, acid-rinsed 10-ml PP tubes (Greiner). After acidification to pH ~ 2 (with cold-distilled 80% HNO_3 ; Suprapur), all samples were stored at 4°C for total and dissolved Fe measurements. Iron was analyzed using a Perkin-Elmer 5100 GF-AAS with a transverse heated graphite tube atomizer (THGA). Samples that contained $<20 \text{ nmol Fe L}^{-1}$ were preconcentrated three times by injecting $20 \mu\text{l}$ of the sample and drying for 50 s at 130°C . The detection limit was 3 nmol L^{-1} for the preconcentrated samples. For every sample, an iron mass balance was established to determine whether iron was gained or lost during fractionation. The DI concentrations were measured for $0.2 \mu\text{m}$ filtered water (Table 1) and for all different DOM fractions (data not shown). The percentage of DI recovered after fractionation from bulk DI ($<0.2 \mu\text{m}$) was calculated as follows:

$\% \text{ DI recovered} = 100 \times (\text{DI}_{\text{retentate}} + \text{DI}_{\text{permeate}}) \times (\text{DI}_{<0.2\mu\text{m}})^{-1}$. The $\text{DI}_{\text{retentate}}$ concentrations were determined by using the concentration factors from DOC mass balances. The DI mass balance calculations revealed recoveries of 45–180% for ultrafiltration and 89–160% for C18 solid phase extraction.

Iron(II) was measured during and after irradiation of the DOM fractions (Figs. 2, 5) by using a flow injection analysis system with luminol-based chemiluminescence detection (FeLume) (Emmenegger et al. 2001). Fe(II) samples were introduced into the flow cell and mixed with an ammonia-buffered luminol reagent. At pH 9.8, Fe(II) is oxidized by oxygen on a millisecond timescale that catalyzes the oxidation of luminol and produces blue, chemiluminescence light.

Hydrogen peroxide (H_2O_2) measurements—Before and at the end of the irradiation, DOM fractions were sampled in duplicates and immediately analyzed. For measuring H_2O_2 , we used the methods of Miller and Kester (1988) and Emmenegger et al. (2001) and used a Perkin-Elmer LS-3 fluorescence spectrophotometer. We also found that the potential light-induced production of organic peroxides did not influence the H_2O_2 fluorescence measurements (data not shown).

Bacterial abundance and biomass production—Samples (10 ml) for microscopy were preserved with a filtered borax-buffered formaldehyde solution (5% final concentration) and stored, refrigerated, in the dark. Bacterial abundance was

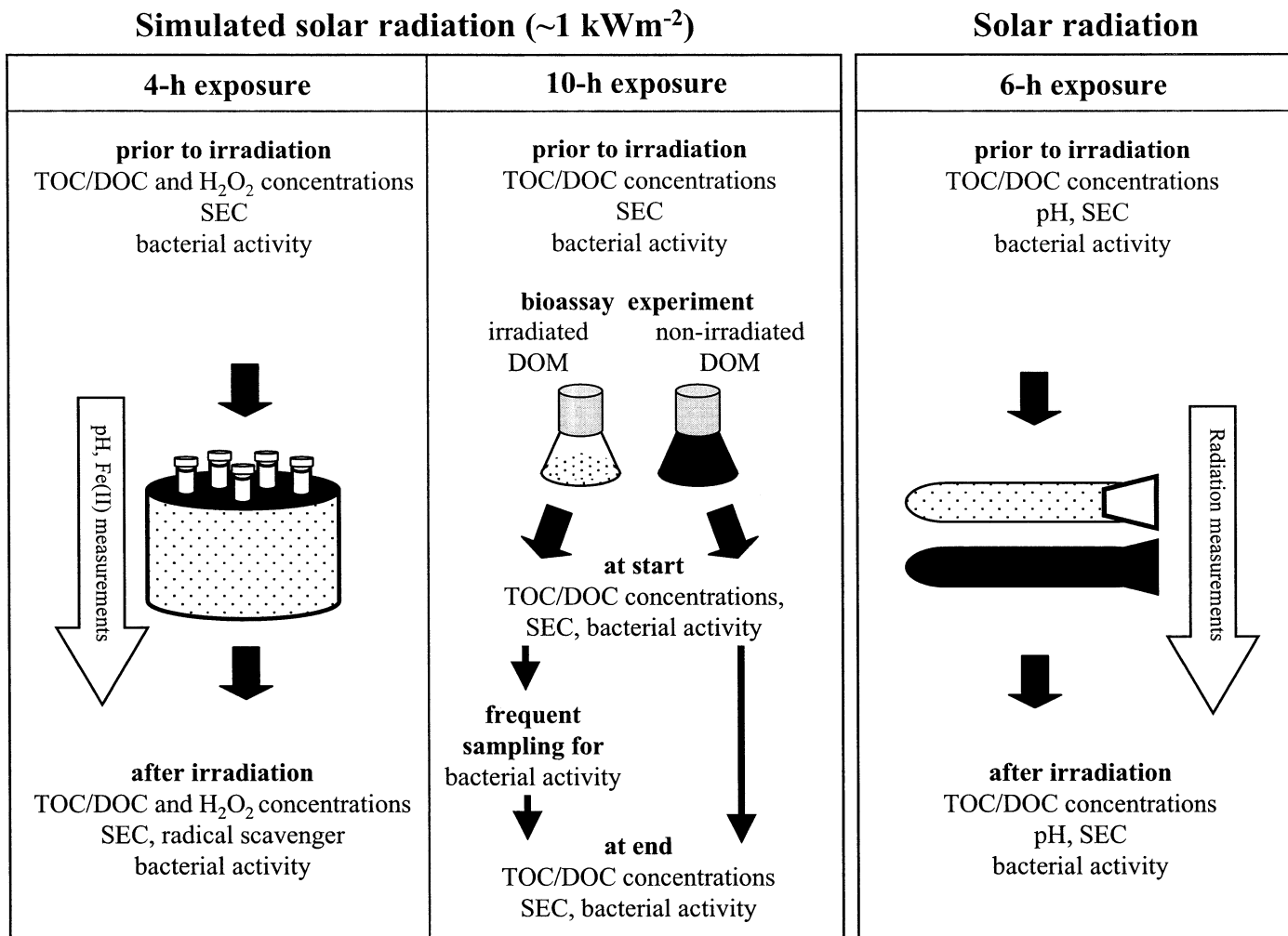


Fig. 2. Scheme of photochemical experiments conducted under laboratory and field conditions.

determined within 2 weeks of sample collection by epifluorescence microscopy (Olympus BX50; magnification, $\times 1,000$) of 4',6-diamidino-2-phenylindole-stained cells (Porter and Feig 1980). In the laboratory and field experiments, the bacterial biomass production was estimated from protein synthesis by adding [^3H]leucine (20 nmol L^{-1} final concentration) to 5-ml samples and incubating them in the dark at 20°C for 60 min (Kirchman et al. 1986). All samples were measured in triplicate with two formaline-killed (2% final concentration) blanks. After incubation, the samples were filtered onto cellulosenitrate filters ($0.2 \mu\text{m}$ pore size, 25 mm diameter, GSWP; Millipore) and rinsed twice with 5 ml of chilled 5% trichloroacetic acid. The filters were placed in scintillation vials with 10 ml of scintillation cocktail (Insta-Gel; Packard) added. Radioactivity was assessed with a liquid scintillation counter (Packard Tri-Carb 2000) by external standard ratio technique. We used the factor $3.1 \mu\text{g C nmol}^{-1}$ leucine for converting leucine incorporation into the bacterial biomass (Simon and Azam 1989). In the following text, bacterial biomass production, which was normalized by bacterial abundance of the individual sample, is used to express bacterial DOM utilization (or bacterial DOM uptake).

Irradiation experiments—In the laboratory, all DOM fractions were irradiated for 4 h with a 1,000 W Xe-lamp (OSRAM; PTI), to simulate a full solar day (Fig. 2). The light intensity was $\sim 1 \text{ kW m}^{-2}$, as determined by ferrioxalate actinometry (Hatchard and Parker 1956). The light was focused by two Pyrex lenses (50% cutoff at 305 nm) and a mirror onto a water-jacketed reactor with a quartz bottom window. A more detailed description of the experimental setup is found in Siffert and Sulzberger (1991). During exposure, the sample was continuously stirred, the temperature was kept constant at 22°C , and the pH was determined with an Orion Ross electrode and an Orion meter calibrated with National Bureau of Standards (NBS) buffers. Before and after irradiation, we sampled for TOC, DOC, SEC, H_2O_2 , and bacterial DOM utilization (Fig. 2). To determine bacterial DOM utilization, a bacterioplankton inoculum at 1:10 dilution was added to the irradiated and nonirradiated DOM fractions, and bacterial abundance and biomass production were determined (see above). Iron(II) concentrations were determined in separate irradiation experiments by use of the FeLume system (see above).

To test the potential effect of ROS on bacterial DOM up-

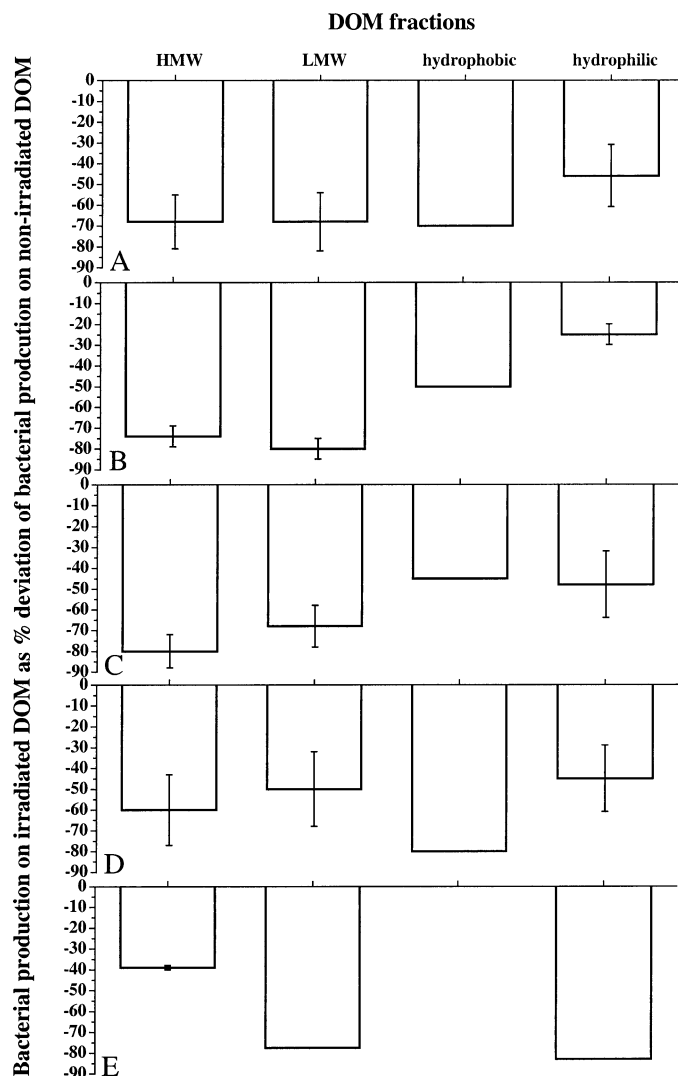


Fig. 3. Decrease (% deviation) in bacterial utilization of irradiated DOM fractions relative to bacterial utilization of nonirradiated DOM fractions at t_0 . DOM originated from the main channel in the (A) headwater, (B) major, and (D) transition floodplain, and (C) from an isolated pool in the major floodplain. The exposure of the DOM fractions to simulated sunlight lasted for 4 h. Panel E shows the decrease in bacterial utilization of DOM fractions irradiated for 6 h under in situ conditions in July and August 2000. DOM utilization expresses bacterial biomass production ($\text{fg C cell}^{-1} \text{d}^{-1}$). Data from panels A–D represent the annual means of 3–6 experiments; vertical bars indicate SEs. Data from panel E represent the mean of 2 experiments; vertical bars indicate the mean deviation.

take in irradiated fractions, samples from March 1999 and April 2000 were split into three aliquots after a 4-h irradiation. Methanol or Trolox C (6-hydroxy-2,5,7,8-tetramethylchroman-2-carboxylic acid; Merck) were added to two aliquots within 60 s after irradiation (Figs. 2, 4) and the third aliquot was left untreated as a control. Methanol exclusively scavenges hydroxyl radicals, and Trolox C, a vitamin E analog, acts as a broadband radical scavenger (Davies et al. 1988). We added methanol to final concentrations of 250–1,000 $\mu\text{mol L}^{-1}$, depending on the DOC concentration of the

sample. Trolox C was added at the much lower concentration of 500 nmol L^{-1} , which corresponds to the average amount of H_2O_2 formed during a 4-h irradiation. Methanol and Trolox C were verified to be nontoxic to bacterial activity in the concentration range that we used. Within 60 s of the addition of methanol or Trolox C to each sample, natural bacterioplankton was added at 1:10 dilution (also to the control without scavenger), to measure bacterial abundance and biomass production (see above).

For long-term bioassay experiments, DOM from April 2000 was irradiated for 10 h (Fig. 2). As mentioned above, before irradiation, HMW and hydrophobic DOM were rediluted with MQ-UV water to a final DOC concentration of $\sim 100 \mu\text{mol C L}^{-1}$. Hydrophilic and LMW DOM were not diluted further and contained DOC concentrations of 27–81 $\mu\text{mol C L}^{-1}$. After the 10-h exposure to simulated sunlight, the samples were transferred to 500-ml Erlenmeyer flasks. Nutrients (30 $\mu\text{mol L}^{-1}$ nitrate and 300 nmol L^{-1} phosphate) were added to the HMW and hydrophobic DOM fractions to levels that had been detected in 0.2 μm of filtered Tagliamento river water (data not shown), followed by the addition of natural bacterioplankton at 1:10 dilution. Except for irradiation, the dark controls were treated identically. The flasks were incubated under light/dark (day/night) conditions at room temperature (22°C) and shaken every 2 h, to prevent nutrient gradient formation. We started to determine bacterial abundance and biomass production immediately after inoculation (t_0), and we kept sampling every ~ 12 h up to a maximum of 100 h. We also sampled for SEC at t_0 and during the steady-state conditions of the bioassay experiments (Figs. 8, 9). Steady-state conditions were estimated from bacterial abundance measurements.

In the field, DOM fractions were exposed under ambient conditions to natural solar radiation during July and August 2000 (Fig. 2). For each DOM fraction, one aliquot was used as a dark control and was placed, bubble-free, in a 120-ml Winkler flask and wrapped in aluminum foil. The other aliquot was placed, bubble-free, in a 120-ml quartz-glass tube with a N/S glass stopper and sealed with Teflon-tape, parafilm, and some textile tape. The tubes and flasks were fixed on a floating mesh and incubated submersed (20 cm) in the surface water of R4 for 6 h (10–16 GMT). During incubation, the surface and underwater solar radiation levels were measured every 3 h with UV-B (290–320 nm), UV-A (320–400 nm), and photosynthetically active radiation (PAR) sensors (SD 104A-COS, SD 104B-COS; Macam) and a LI-COR 1000 data logger. Before and after irradiation, we sampled for TOC, DOC, iron, and bacterial activity.

Results and discussion

Carbon and iron concentrations in the various DOM fractions—In the Tagliamento River, the dominant form of organic carbon was DOC, with average concentrations of 10–91 $\mu\text{mol C L}^{-1}$ (Table 1). DOC and particulate organic carbon (POC) concentrations were low and comparable to other highly oligotrophic surface waters (Benner et al. 1997; Tockner et al. 2002). POC concentrations were calculated as the difference between TOC and DOC values and increased

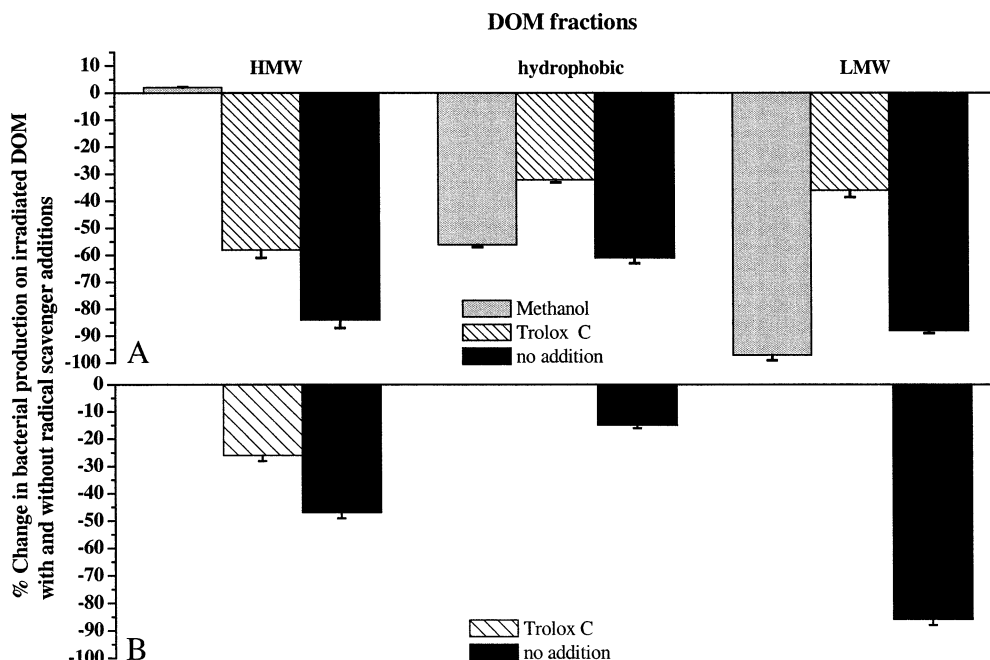


Fig. 4. Effects of methanol and Trolox C on bacterial utilization of irradiated HMW, LMW, and hydrophobic fractions sampled in April 2000 (A) directly after irradiation and (B) after 2 h in the dark. Methanol was added at concentrations of 250–1,000 $\mu\text{mol L}^{-1}$ and Trolox C at 500 nmol L^{-1} . DOM utilization is expressed by bacterial biomass production ($\text{fg C cell}^{-1} \text{d}^{-1}$). The change in bacterial utilization of irradiated DOM fractions with and without radical scavenger additions is calculated as % deviation of utilization of nonirradiated DOM. Data points represent the mean of 2–3 measurements; vertical bars indicate the standard error or mean deviation.

from 1% to 10% of the TOC along the main channel. These percentages are very low relative to stream size (Meybeck 1981). We observed this dominance of DOM throughout the seasons, even during postflood conditions in August 1999. Although high loads of inorganic carbon (carbonate and dolomite) were transported after flooding, 90% of organic carbon was still present as DOC. During the year, only 8–29% and 13–54% of DOM were retained by ultrafiltration and C18-solid phase extraction, respectively, comparable to that reported for oligotrophic marine waters (Amador et al. 1990; Benner et al. 1997). The major portion of DOM consisted of hydrophilic, LMW compounds (data not shown).

Iron was abundant in the water column of the Tagliamento River. In the main channel, 91–94% of iron was present in the particulate and colloidal phase and did not pass through a 0.2- μm filter. The remaining 6–9% iron was associated with DOM. Its distribution compares well to other freshwater systems (Emmenegger et al. 2001). In the isolated pool, located within a large island of the major floodplain, we found, on average, only 19% of iron in the particulate and colloidal phase. It seems that massive groundwater upwelling, infiltration by the carbonaceous substrate (gravel), and autochthonous algal production may change particle composition in the pool compared with that in the MC system. Over the year, DI concentrations in 0.2- μm filtered river water samples were 3–57 nmol L^{-1} (data not shown). Concerning the distribution of iron in the different DOM fractions, we found that most of the DI ($65 \pm 4\%$, average \pm SE, $n = 21$) was contained in LMW and hydrophilic DOM

throughout the year. Only in April 2000 was a surplus of iron associated with HMW and hydrophobic DOM ($56 \pm 8\%$, $n = 8$).

Short-term effect of DOM irradiation on bacterial DOM utilization—Bacterial biomass production on irradiated DOM fractions was measured immediately after a 4-h exposure to simulated sunlight. Bacterial cells were incubated for 1 h with each DOM fraction in the dark. The short-term DOM utilization of all irradiated DOM fractions decreased by up to 80%, compared with the short-term uptake of nonirradiated DOM (Fig. 3). We found the same trend for all samples from the MC and isolated pool and throughout the year, which may reflect a minimal spatiotemporal variability of the chemical composition of DOM in this river (unpubl. data).

We also found the same level of inhibition during field studies in July and August 2000 (Fig. 3E). To simulate a full solar day, we exposed the DOM fractions, submersed (20 cm) in surface river water, to sunlight for 6 h. Surface irradiation levels were comparable to values found in the literature (Herndl et al. 1993), and, at the maximum, were 5 W m^{-2} for UV-B (290–320 nm), 82 W m^{-2} for UV-A (320–400 nm), and 461 W m^{-2} for PAR (400–700 nm). In the top 20 cm of the water column, the attenuation of sunlight was within 25% for UV-B, 23% for UV-A, and 10% for PAR.

Because sunlight may also directly affect bacterioplankton by damaging cell physiology and DNA (Herndl et al. 1993; Jeffrey et al. 1996), we additionally tested the direct effect

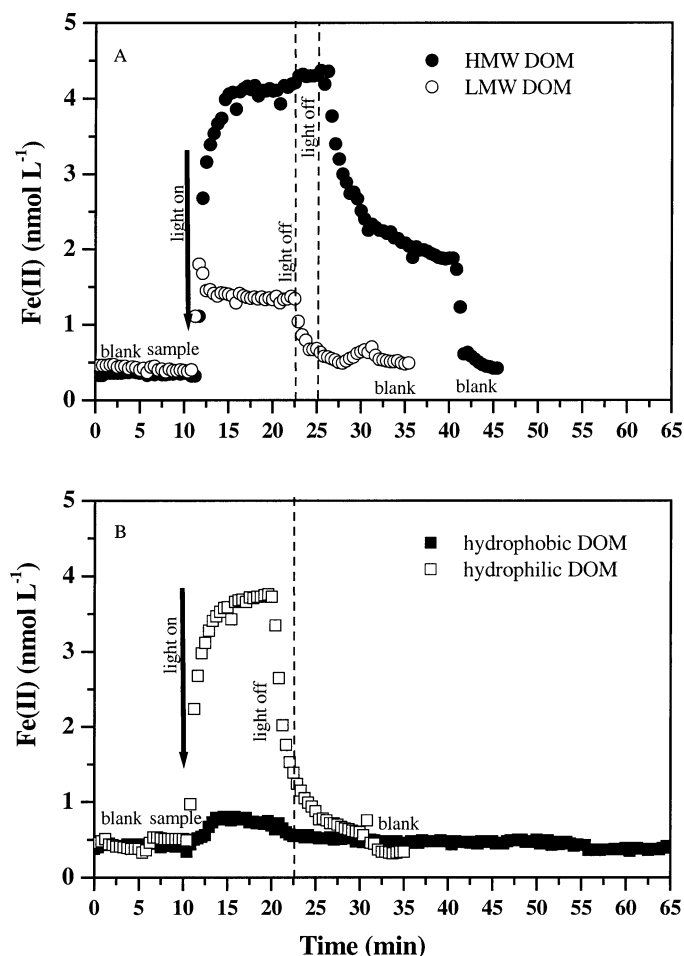


Fig. 5. Concentrations of Fe(II) during irradiation and after the light source was turned off in HMW and LMW DOM and hydrophobic and hydrophilic DOM fractions. "Blank" indicates measurement of MQ-UV water at pH ~ 9 (pH raised by adding a 25% ammonia solution) before and after sample measurement. Dashed lines indicate when the simulated sunlight was switched off. Fe(II) was measured by chemiluminescence detection (FeLume). We used different calibrations curves for low and higher Fe(II) concentrations.

of solar radiation on bacterioplankton activity. We exposed raw water samples (DOM and bacteria) and 0.2- μm filtered samples (only DOM) to simulated sunlight for 4 h, and then introduced a natural bacterioplankton inoculum to the filtered nonirradiated and irradiated water samples. For both raw and filtered, irradiated water samples, we measured a strong decrease in bacterial DOM utilization (relative to nonirradiated DOM), and the inhibition was only slightly greater for irradiated raw water samples (data not shown). These additional experiments indicated that the direct photoinhibition of bacterial cells was negligible, but DOM transformation and the concomitant production of reactive species were mostly responsible for the decrease in bacterial DOM utilization.

To test the effect of ROS on bacterial activity, we conducted experiments with two different scavengers of ROS, methanol and Trolox C. The scavengers were added to the

DOM immediately after the light source was turned off, followed by inoculation of a natural bacterioplankton community. Only for HMW DOM was methanol effective at preventing a decrease in DOM utilization (Fig. 4A). On the basis of this result, we hypothesize that HO^\bullet or organic peroxy radicals formed in the Fenton reaction and in subsequent thermal reactions of HO^\bullet with HMW DOM compounds are responsible for the inhibition in bacterial uptake of HMW DOM.

To test whether the Fenton reaction could play an important role in our systems, we measured ambient Fe(II) concentrations in the DOM fractions during and after irradiation. Irradiation of the DOM fractions led to the formation of Fe(II), and steady-state concentrations were reached between 1 and 5 min, depending on the individual DOM fraction (Fig. 5). The highest $[\text{Fe(II)}]_{\text{ss}}$ levels were detected in irradiated HMW DOM, followed by hydrophilic, LMW, and hydrophobic DOM (Fig. 5, Table 1). (Note that the numbers listed in Table 1 are average $[\pm \text{SE}]$ values from seasonally collected samples). Mean $[\text{Fe(II)}]_{\text{ss}}$ levels, normalized to DOC concentration, were higher by a factor of 4.6 in HMW and hydrophilic than in LMW and hydrophobic DOM (Table 1). The percentages of $[\text{Fe(II)}]_{\text{ss}}$ from DI contained in the individual fractions also were generally higher in HMW and hydrophilic DOM.

Regarding the kinetics of Fe(II) formation and its decay in the HMW fraction, the following observation was striking: When we turned off the light, we found that, despite a pH ~ 8.1 , $[\text{Fe(II)}]_{\text{ss}}$ only gradually decreased, and a new Fe(II) steady state was established (Fig. 5A). This phenomenon has also been observed in irradiated, unfiltered water samples from a Swiss lake (Emmenegger et al. 2001). Those authors were able to get excellent agreement between their experimental data and mathematical kinetic modeling by involving continuous redox cycling of iron after irradiation, with Fe(III) being re-reduced by the superoxide radical ($\text{O}_2^{\bullet -}$) formed in the oxidation of Fe(II) by O_2 (Voelker and Sedlak 1995; Emmenegger et al. 2001). An alternative explanation for the slow decay of Fe(II) after irradiation would be stabilization of Fe(II) by an organic ligand contained in the HMW fraction. The pronounced effect of excess methanol on bacterial utilization of irradiated HMW DOM, however, suggests continuous formation of HO^\bullet after irradiation, via the Fenton reaction, although with low yields at pH 8.1 (S. J. Hug and O. Leupin unpubl. data).

In the presence of Trolox C, the bacterial uptake of irradiated HMW DOM was still much lower than in the nonirradiated sample (Fig. 4A), although Trolox C is an efficient scavenger of HO^\bullet (the second-order rate constant of reaction with HO^\bullet is $\sim 2.2 \times 10^9 \text{ mol}^{-1} \text{ s}^{-1}$ for Trolox C at pH 7 [Davies et al. 1988] and $\sim 7.9 \times 10^8 \text{ mol}^{-1} \text{ s}^{-1}$ for methanol [Buxton et al. 1988]). This result may be explained by the fact that the concentration of Trolox C was too low (see "Materials and methods") to scavenge the total amount of ROS, including HO^\bullet . In the irradiated hydrophobic and LMW fractions, Trolox C also diminished the inhibition of bacterial production relative to samples without scavenger additions. Of interest, methanol showed no effect in these fractions (Fig. 4A). From this result, we conclude that other ROS, possibly organic peroxides, may evolve from the pho-

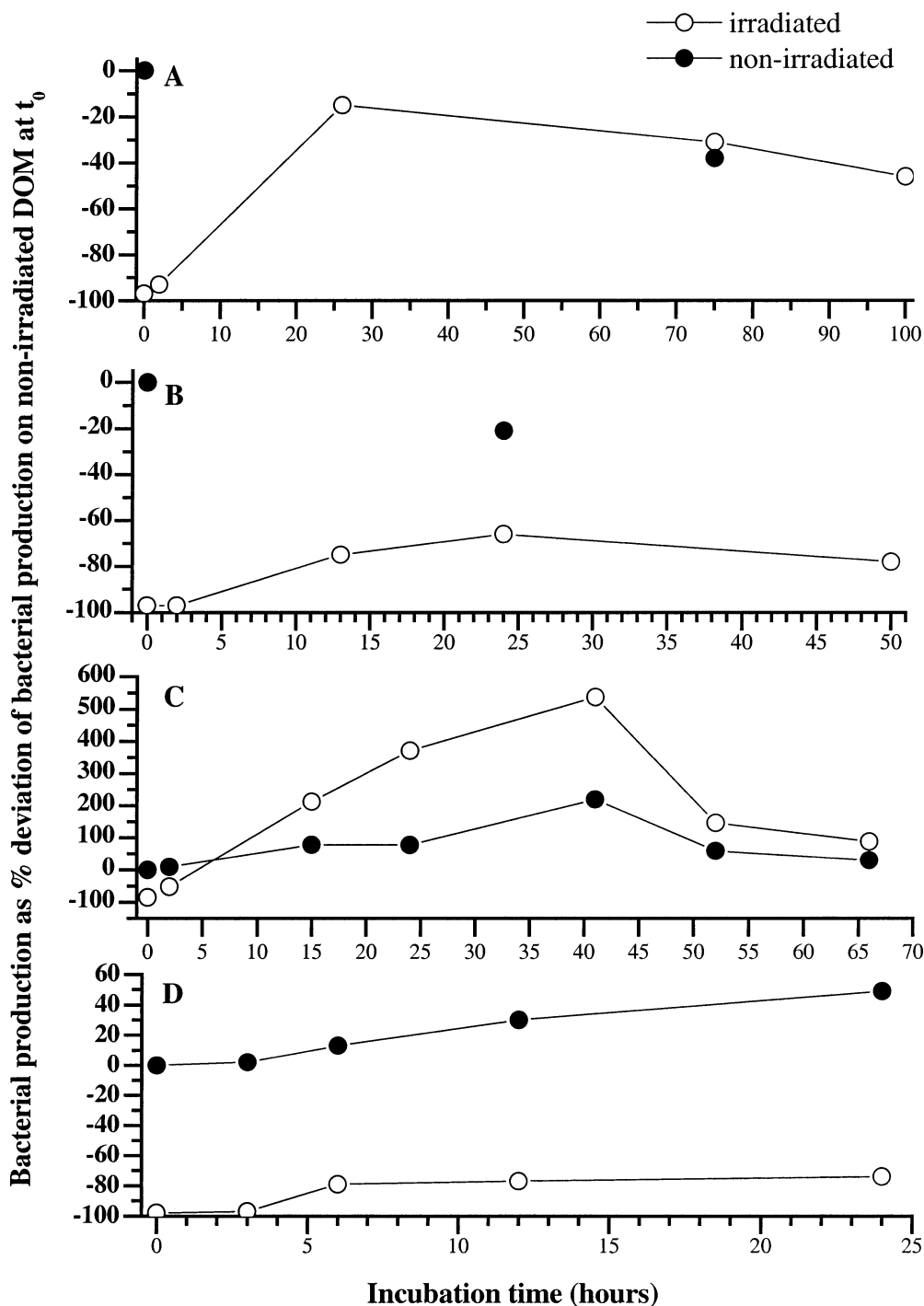


Fig. 6. Long-term bioassay experiments on irradiated and nonirradiated DOM fractions sampled during April 2000: (A) HMW, (B) LMW, (C) hydrophobic, and (D) hydrophilic DOM. Bacterial DOM utilization is expressed by measuring bacterial biomass production ($\text{fg C cell}^{-1} \text{d}^{-1}$). Changes in bacterial DOM utilization are calculated as % deviation of utilization of nonirradiated DOM before long-term incubation.

tochemical transformations of hydrophobic and LMW DOM. Note that H_2O_2 at concentrations of 50–400 nmol L^{-1} (Table 1) did not affect bacterial activity (data not shown).

To test the effect of DOM irradiation on bacterial DOM utilization over longer time periods, we left the irradiated

fractions for 2 h in the dark and then added a bacterioplankton inoculum. In the HMW and hydrophobic fractions, the inhibition of bacterial DOM uptake had diminished after 2 h, compared with DOM utilization immediately after irradiation. However, this did not occur in the LMW fraction

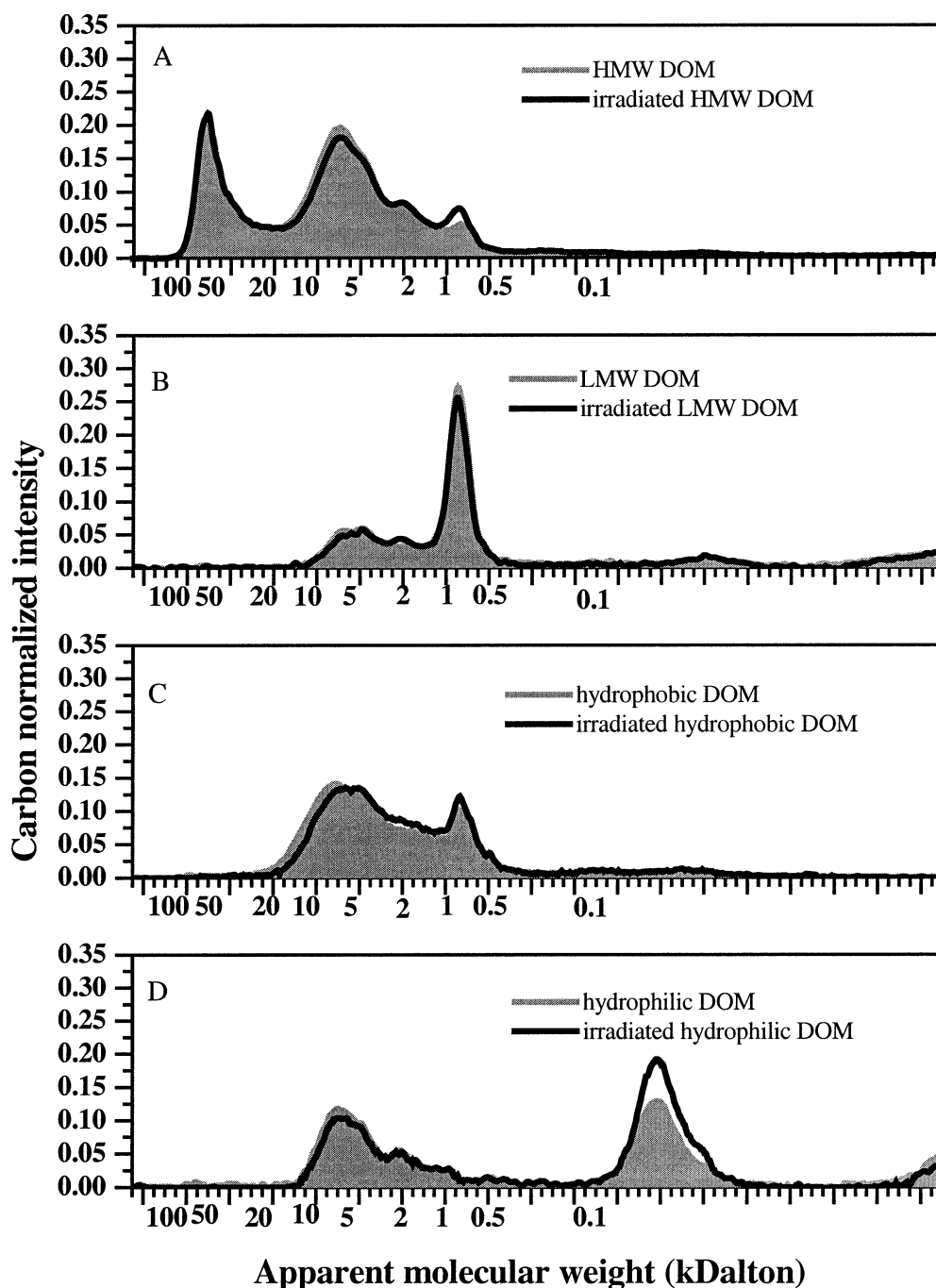


Fig. 7. Size exclusion chromatograms of nonirradiated (A) HMW, (B) LMW, (C) hydrophobic, and (D) hydrophilic DOM. Solid lines represent apparent molecular weight distributions after a 10-h irradiation with simulated sunlight ($\sim 1 \text{ kW m}^{-2}$).

(Fig. 4A,B). In a further experiment, we added Trolox C to one of the two irradiated HMW DOM samples, left it for 2 h in the dark, and then measured the bacterial DOM uptake. As Fig. 4B shows, Trolox C had a positive effect on bacterial DOM uptake even when it was added 2 h after irradiation. These results suggest that ROS are formed in the dark, after irradiation, over longer time periods, but with a decreasing effect on bacterial DOM utilization. The results shown in

Fig. 4B also indicate that changes of DOM bioavailability on DOM photo-oxidation are different for different fractions.

Long-term effect of DOM irradiation on bacterial DOM utilization—To compare long-term bacterial growth on non-irradiated and irradiated DOM sources, we incubated bacterioplankton from the Tagliamento River with nonirradiated and irradiated HMW, LMW, hydrophobic, and hydrophilic

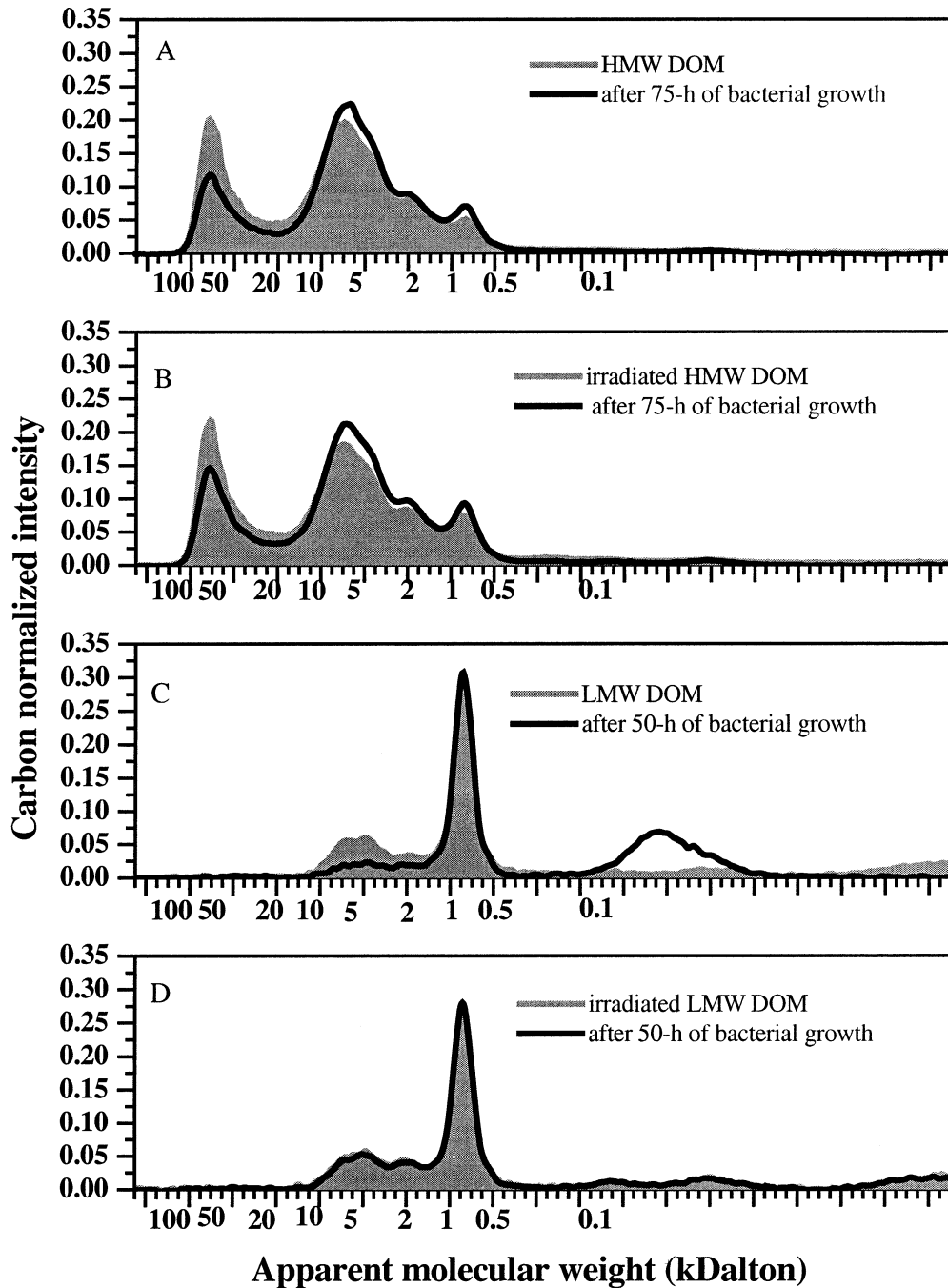


Fig. 8. Size exclusion chromatograms of HMW DOM (A) before and (B) after 10 h of irradiation and LMW DOM (C) before and (D) after 10 h of irradiation with simulated sunlight ($\sim 1 \text{ kW m}^{-2}$). The solid lines represent apparent molecular-weight distributions after 75 h of bacterial growth on (A) nonirradiated and (B) irradiated HMW DOM and after 50 h of bacterial growth on (C) nonirradiated and (D) irradiated LMW DOM. The samples were collected from the bioassay experiments after bacterial growth had reached steady state (see Fig. 6A,B).

DOM. Before inoculation with bacterial cells, the four DOM fractions were exposed to simulated sunlight for 10 h. In all bioassays, cell growth (bacterial abundance and biomass production) was monitored until and after steady-state conditions were reached (Fig. 6). In these experiments, we also used incubations of 1 h with radioactively labeled leucine to

measure bacterial biomass production, taking measurements at specific time intervals throughout the bioassay experiments (Fig. 6).

Immediately after the exposure of the DOM fractions to simulated sunlight (t_0 in Fig. 6), bacterial DOM utilization was strongly inhibited in irradiated fractions. With ongoing

incubation (over days), this inhibition diminished and bacteria grew at different rates in the different fractions. Bacterial utilization of irradiated compared with nonirradiated DOM was similar for HMW DOM after 75 h (Fig. 6A), considerably higher for hydrophobic DOM after 50 h (Fig. 6C), and severely lower for LMW and hydrophilic DOM after 65 and 25 h, respectively (Fig. 6B,D). These results suggest that HMW and hydrophobic DOM, which were found to be biorecalcitrant in the Tagliamento River (data not shown), stayed unchanged or became more bioavailable on exposure to light. To the contrary, LMW and hydrophilic DOM, which were most abundant and strongly supported bacterial activity in Tagliamento surface waters (data not shown), turned highly biorecalcitrant on irradiation. Of interest, we found higher net rates of H_2O_2 formation (during a 4-h irradiation) in the LMW and hydrophilic fractions than in the HMW and hydrophobic fractions, which suggests that the fractions that turned biorecalcitrant on irradiation are photochemically more reactive in terms of H_2O_2 formation. This trend was independent of the season, with average net rates of H_2O_2 formation being 3 times higher in LMW than in HMW DOM and 5.8 times higher in hydrophilic than in hydrophobic DOM (Table 1).

To elucidate light-induced transformations of the different DOM fractions, we measured the molecular weight distributions of the DOM fractions before and after irradiation for 10 h (Fig. 7). As shown in the figure, irradiation did not result in major shifts in the size spectra. However, for all fractions, irradiation caused the transformation of compounds with apparent molecular weight distributions peaking ~5–10 kDa to products with lower apparent molecular weights.

We also measured the molecular weight distribution after incubation of the fractions with bacterioplankton from the Tagliamento River (Figs. 8, 9). The size-exclusion chromatograms of irradiated and nonirradiated HMW DOM before and after incubation with bacterioplankton showed that cells preferred to utilize large compounds (100–10 kDa) even in the irradiated HMW fraction. This contradicts data from the literature that report the photochemical release of bioavailable substrates with lower molecular weights from recalcitrant freshwater DOM (Wetzel et al. 1995).

Nonirradiated LMW DOM dominantly supported bacterial activity and exhibited low turnover times (data not shown). Surprisingly, bacteria only consumed the larger compounds (10–1 kDa) from this fraction and produced very small compounds, <0.1 kDa in size (Fig. 8C). On irradiation, this material turned highly biorecalcitrant, as reflected by unchanged size spectrum and signal intensity in the irradiated sample after 50 h of bacterial growth (Fig. 8D). The inhibition of bacterial DOM utilization may specifically be associated with the phototransformations of the 10–1-kDa compounds, because their uptake ceased after irradiation. Because of high initial bioavailability and to the very low average C:N ratio (5) of LMW DOM (unpubl. data), we assume that this fraction contains an abundance of amides, aminosugars, and oligosaccharides. The photodigestion of peptides has already been shown to result in a decrease in its bioavailability (Naganuma et al. 1996).

Bacterial growth on nonirradiated and irradiated hydro-

phobic DOM caused no change in the molecular weight distribution of both fractions, but a strong decline in signal intensity was seen in the irradiated fraction (Fig. 9A,B). Therefore, nonirradiated and irradiated DOM after bacterial growth only differed in the extent of decrease in signal intensity. Bacterial activity measurements showed that the turnover of nonirradiated hydrophobic material was low over the course of 43 h (Fig. 6C). Because of exposure to light, this material became more bioavailable, which confirms the results obtained with the bioassay experiments (Fig. 6C).

Bacterial growth on nonirradiated hydrophilic DOM revealed no discernable removal of this material, but, of interest, a production of very small compounds sized <0.1 kDa (Fig. 9C). When bacteria utilized irradiated hydrophilic DOM, they also caused a release of very small compounds (Fig. 9D). Like LMW material, hydrophilic DOM exhibits a low average C:N ratio (3.3), which suggests the presence of proteinaceous matter. We assume that these compounds were easily hydrolyzed at low pH (required for C18 solid-phase extraction) and that the smaller products contributed to the proteinaceous material expected to occur in both fractions. As mentioned above, the photodecomposition of this material may explain the strong decrease in its bioavailability (see Fig. 6D).

Importance of sunlight and iron for riverine carbon cycling—Natural rivers like the Tagliamento River that exhibit low TOC concentrations (<100 $\mu\text{mol C L}^{-1}$) show low light attenuation with depth, and the water column receives high doses of solar radiation over the year. The Tagliamento preserves >60% of its aerial extension in the form of nonperturbed still water or slow-flowing water bodies (van der Nat 2002), which have an average depth of only 0.5 m (unpubl. data). For this reason, high percentages of sunlight can penetrate to bottom levels in the majority of different aquatic habitats in the Tagliamento ecosystem, causing photochemical transformations of DOM and the light-induced redox cycling of iron. Thereby, ROS are formed that greatly affect bacterial DOM utilization.

In the Tagliamento River, DOM undergoes severe photochemical transformations that ultimately determine the long-term growth of bacteria on these phototransformed energy sources. The chemical reactions involved appear to be strongly dependent on the chemical composition of riverine DOM. Previous studies have shown that HMW and hydrophobic components likely derive from the leaching of soils that contain highly altered plant material and prokaryotic biomass (Kaiser et al. 2003). Its origin helps to explain why this material behaves in a manner recalcitrant to bacterial utilization. On the contrary, LMW and hydrophilic components potentially derive from the decomposition of “young,” fine particulate organic matter and autochthonous microalgae biomass. This pool of molecules shows low C:N ratios (3–5) and may explain why they are highly bioavailable to the bacterioplankton community (see above). Taking all DOM fractions, in Tagliamento waters, dominantly large (100–20 kDa) and smaller (~1 kDa), possibly highly diagenetically altered, compounds exhibit low photoreactivity and therefore show no change in bioavailability on irradiation. Some constituents of hydrophobic DOM are photoreactive and become

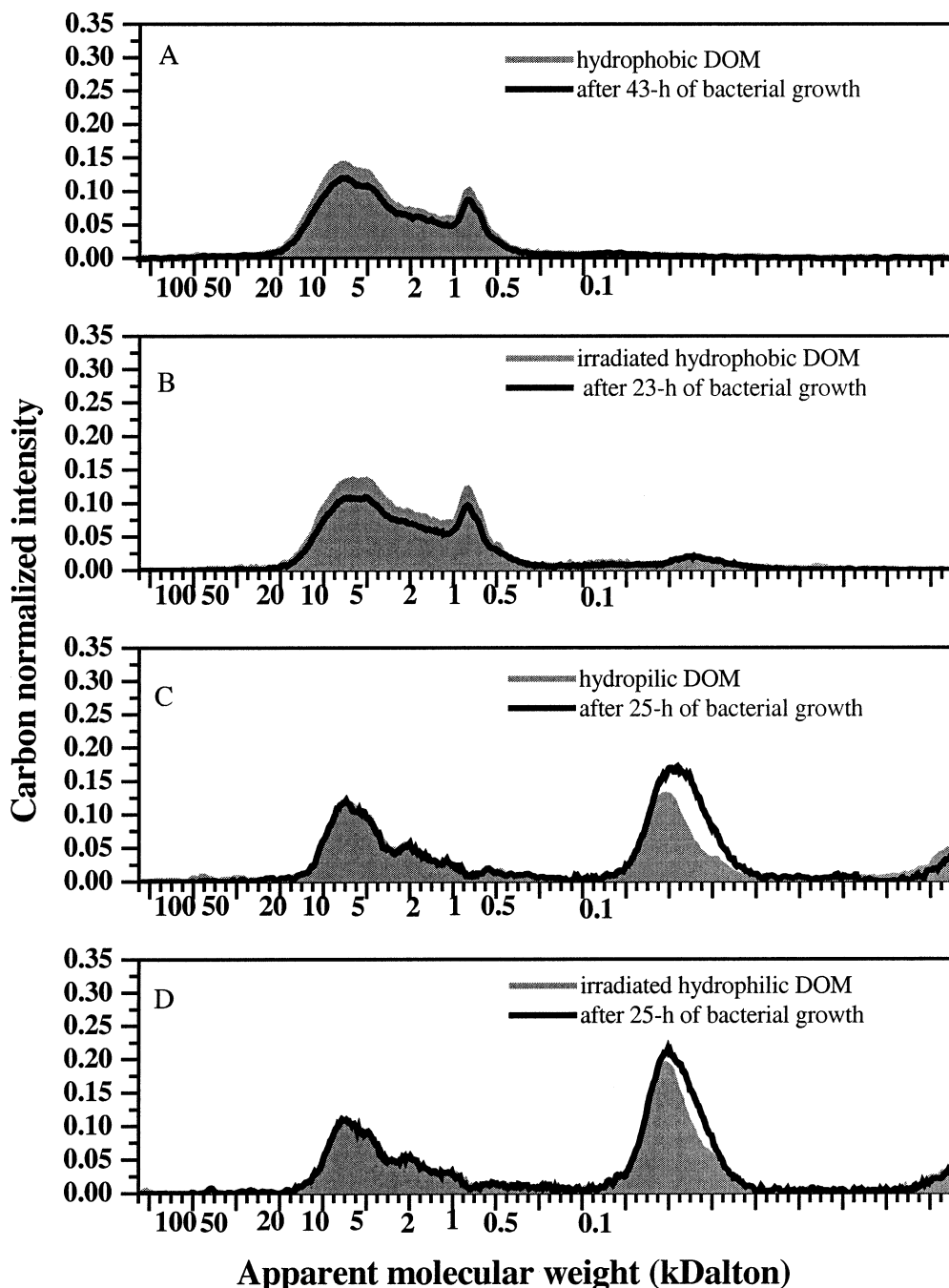


Fig. 9. Size exclusion chromatograms of hydrophobic DOM (A) before and (B) after 10 h of irradiation and hydrophilic DOM (C) before and (D) after 10 h of irradiation with simulated sunlight ($\sim 1 \text{ kW m}^{-2}$). The solid lines represent apparent molecular weight distributions after 43 h of bacterial growth on (A) nonirradiated and 23 h of bacterial growth on (B) irradiated hydrophobic DOM and after 25 hours of bacterial growth on (C) nonirradiated and (D) irradiated hydrophilic DOM. The samples were collected from the bioassay experiments after bacterial growth had reached steady state (see Fig. 6C,D).

highly bioavailable on irradiation. Larger components of LMW and hydrophilic DOM are also photoreactive, however, becoming highly biorecalcitrant when exposed to light in surface waters.

We confirm the findings in the literature (Benner and Bidanda 1998; Obernosterer et al. 1999) that light can have

contrasting effects on natural DOM, turning bioactive into biorecalcitrant compounds and vice versa. Such phototransformations are highly critical for our river system because they decrease the bioavailability of the major important energy sources for the bacterioplankton community. As a consequence, this effect measured along the river continuum

suggests an accumulation of biorecalcitrant compounds and, hence, increasing nutritional limitation for bacteria with downstream transport and the diminishing microbial reworking of DOM. For the Tagliamento River system, we therefore propose a light-induced shift from microbial transformation processes of bioavailable substrates to the hydrological transport of photochemically altered and biorecalcitrant DOM. Others have reported that chemical, physical, and microbial reworking longitudinally decreases the nutritional value of DOM (Vannote et al. 1981; Hedges et al. 1994). Ours is the first study to show how light longitudinally affects the microbial turnover of DOM and continuously contributes to the transformation of organic compounds along the river continuum. However, many questions still need to be answered regarding the photochemical transformations of organic compounds. For future research, it would be highly rewarding to trace the light-induced structural changes in specific DOM compounds, such as bioavailable and biorecalcitrant substrates. The chemical characterization of organic ligands forming complexes with metals also would be key for understanding the light-induced redox cycling of metals in natural waters and their potential relationships with DOM bioavailability. Elucidating the different reactive species involved would result in a more complete picture of photochemical transformations in freshwater systems.

References

- AMADOR, J. A., P. J. MILNE, C. A. MOORE, AND R. G. ZIKA. 1990. Extraction of chromophoric humic substances from seawater. *Mar. Chem.* **29**: 1–17.
- AMON, R. M. W., AND R. BENNER. 1996. Photochemical and microbial consumption of dissolved organic carbon and dissolved oxygen in the Amazon River system. *Geochim. Cosmochim. Acta* **60**: 1783–1792.
- BENNER, R., AND B. BIDDANDA. 1998. Photochemical transformations of surface and deep marine dissolved organic matter: Effects on bacterial growth. *Limnol. Oceanogr.* **43**: 1373–1378.
- , B. BLACK, AND M. MCCARTHY. 1997. Abundance, size distribution, and stable carbon and nitrogen isotopic composition of marine organic matter isolated by tangential-flow ultrafiltration. *Mar. Chem.* **57**: 243–263.
- , AND M. STROM. 1993. A critical evaluation of the analytical blank associated with DOC measurements by high-temperature catalytic oxidation. *Mar. Chem.* **41**: 153–160.
- BLOUGH, N. V., AND R. G. ZEPP. 1995. Reactive oxygen species in natural waters, p. 280–333. *In* L. S. Foote, S. S. Valentine, A. Greenbaerg, and S. F. Liebman [eds.], *Active oxygen: Reactive oxygen species in chemistry*. Chapman and Hall.
- BUSHAW, K. L., AND OTHERS. 1996. Photochemical release of biologically available nitrogen from aquatic dissolved organic matter. *Nature* **381**: 404–407.
- BUXTON, G. V., C. L. GREENSTOCK, W. P. HELMAN, AND A. B. ROSS. 1988. Critical review of rate constants of reactions of hydrated electrons, hydrogen atoms and hydroxyl radicals (OH/O⁻) in aqueous solution. *J. Phys. Chem. Ref. Data* **17**: 513–886.
- CHOW, C. K. 1988. Cellular antioxidant defense mechanism, vol. 2. CRC.
- CLAIR, T. A., AND B. G. SAYER. 1997. Environmental variability in the reactivity of freshwater dissolved organic carbon to UV-B. *Biogeochemistry*. **36**: 89–97.
- COTNER, J. B., AND R. T. HEATH. 1990. Iron-redox effects on photosensitive phosphorus release from dissolved humic materials. *Limnol. Oceanogr.* **35**: 1175–1181.
- DAVIES, M. J., FORNI, L. G., AND WILLSON, R. L. 1988. Vitamin E analogue Trolox C. E. *Geochem. J.* **25**: 513–522.
- EMMENEGGER, L., D. W. KING, L. SIGG, AND B. SULZBERGER. 1998. Oxidation kinetics of Fe(II) in a eutrophic Swiss lake. *Environ. Sci. Tech.* **32**: 2990–2996.
- , R. SCHOENENBERGER, L. SIGG, AND B. SULZBERGER. 2001. Light-induced redox cycling of iron in circumneutral lakes. *Limnol. Oceanogr.* **46**: 49–61.
- FRIDOVICH, I. 1986. Biological effects of the superoxide radical. *Arch. Biochem. Biophys.* **247**: 1–11.
- GOLDSTONE, J. V., AND B. M. VOELKER. 2000. Chemistry of superoxide radical in seawater: CDOM associated sink of superoxide in coastal waters. *Environ. Sci. Technol.* **34**: 1043–1048.
- HATCHARD, C. G., AND A. C. PARKER. 1956. A sensitive chemical actinometer. II potassium ferrioxalate as a standard chemical actinometer. *Proc. R. Soc. Lond. Ser. A*: 518–536.
- HEDGES, J. I., G. L. COWIE, J. E. RICHEY, P. D. QUAY, R. BENNER, M. STROM, AND B. R. FORSBERG. 1994. Origins and processing of organic matter in the Amazon River as indicated by carbohydrates and amino acids. *Limnol. Oceanogr.* **39**: 743–761.
- , R. G. KEIL, AND R. BENNER. 1997. What happens to terrestrial organic matter in the ocean? *Org. Geochem.* **27**: 195–212.
- HERNDL, G. J., G. MUELLER-NIKLAS, AND J. FRICK. 1993. Major role of ultraviolet-B in controlling bacterioplankton growth in the surface layer of the ocean. *Nature* **361**: 717–719.
- HUBER, S. A., AND F. H. FRIMMEL. 1992. A liquid chromatographic system with multi-detection for the direct analysis of hydrophilic organic compounds in natural waters. *Fresenius J. Anal. Chem.* **342**: 198–200.
- JEFFREY, W. H., R. J. PLEDGER, P. AAS, S. HAGER, R. B. COFFIN, R. VAN HAVEN, AND D. L. MITCHELL. 1996. Diel and depth profiles of DNA photodamage in bacterioplankton exposed to ambient solar radiation. *Mar. Ecol. Prog. Ser.* **137**: 293–304.
- JOHANNSSON, S. C., AND W. L. MILLER. 2001. Quantum yields for the photochemical production of dissolved organic carbon in seawater. *Mar. Chem.* **76**: 271–283.
- KAISER, E., A. J. SIMPSON, K. J. DRIA, B. SULZBERGER, AND P. G. HATCHER. 2003. Solid-state and multidimensional solution-state NMR of solid phase extracted and ultrafiltered riverine dissolved organic matter (DOM). *Environ. Sci. Technol.* **37**: 2929–2935.
- KIEBER, D. J., J. MCDANIEL, AND K. MOPPER. 1989. Photochemical source of biological substrates in sea water: Implications for carbon cycling. *Nature* **341**: 637–639.
- KIRCHMAN, D. L., S. Y. NEWELL, AND R. E. HODSON. 1986. Incorporation versus biosynthesis of leucine: Implications for measuring rates of protein synthesis and biomass production by bacteria in marine systems. *Mar. Ecol. Prog. Ser.* **32**: 47–59.
- LOUCHOUARN, P., S. OPSAHL, AND R. BENNER. 2000. Isolation and quantification of dissolved lignin from natural waters using solid-phase extraction and GC/MS. *Anal. Chem.* **72**: 2780–2787.
- MEYBECK, M. 1981. Carbon, nitrogen, and phosphorous transport by world rivers. *Am. J. Sci.* **282**: 401–450.
- MILES, C. J., AND BREZONIK, P. L. 1981. Oxygen consumption in humic-colored waters by a photochemical ferrous-ferric catalytic cycle. *Environ. Sci. Technol.* **15**: 1089–1095.
- MILLER, W. L., AND D. R. KESTER. 1988. Hydrogen measurement in seawater by (p-hydroxyphenyl) acetic acid dimerization. *Anal. Chem.* **60**: 2711–2715.
- MOFFETT, J. W., AND R. G. ZIKA. 1987. Reaction kinetics of hydrogen peroxide with copper and iron in seawater. *Environ. Sci. Technol.* **21**: 804–810.
- MUELLER, M. B., D. SCHMITT, AND F. H. FRIMMEL. 2000. Fraction-

- ation of Natural organic matter by size exclusion chromatography properties and stability of fractions. *Environ. Sci. Technol.* **34**: 4867–4872.
- NAGANUMA, T., S. KONISHI, T. INOUE, T. NAKANE, AND S. SUKIZAKI. 1996. Photodegradation or photoalteration? Microbial assay of the effect of UV-B on dissolved organic matter. *Mar. Ecol. Prog. Ser.* **135**: 309–310.
- OBERNOSTERER, I., B. REITNER, AND G. J. HERNDL. 1999. Contrasting effects of solar radiation on dissolved organic matter and its bioavailability to marine bacterioplankton. *Limnol. Oceanogr.* **44**: 1645–1654.
- OPSAHL, S., AND R. BENNER. 1998. Photochemical reactivity of dissolved lignin in river and ocean waters. *Limnol. Oceanogr.* **43**: 1297–1304.
- PERMINKOVA, I. V., F. H., FRIMMEL, D. V. KOVALEVSKII, G. ABBT-BRAUN, A. V. KUDRYAVTSEV, AND S. HESSE. 1998. Development of a predictive model for calculation of molecular weight of humic substances. *Wat. Res.* **32**: 872–881.
- PORTER, K. G., AND T. S. FEIG. 1980. The use of DAPI for identifying and counting aquatic microflora. *Limnol. Oceanogr.* **25**: 943–948.
- RAYMOND, P. A., AND J. E. BAUER. 2001. Riverine export of aged terrestrial organic matter to the North Atlantic Ocean. *Nature* **409**: 497–500.
- SCHLESINGER, W. H., AND J. M. MELACK. 1981. Transport of organic carbon in the world's rivers. *Tellus* **33**: 172–187.
- SIFFERT, C., AND B. SULZBERGER. 1991. Light-induced dissolution of hematite in the presence of oxalate: A case study. *Langmuir* **7**: 1627–1634.
- SIMON, M., AND F. AZAM. 1989. Protein content and protein synthesis rates of planktonic marine bacteria. *Mar. Ecol. Prog. Ser.* **51**: 201–213.
- TOCKNER, K., F. MALARD, U. UEHLINGER, AND J. V. WARD. 2002. Nutrients and organic matter in a glacial river-floodplain system (Val Roseg, Switzerland). *Limnol. Oceanogr.* **47**: 266–277.
- VAN DER NAT, D. 2002. Ecosystem processes in the dynamic Tagliamento River. Ph.D. thesis, Swiss Federal Institute of Technology, Zurich.
- VANNOTE, R. L., G. W. MINSHALL, K. W. CUMMINS, J. R. SEDELL, AND C. E. CUSHING. 1980. The river continuum concept. *Can. J. Fish. Aquat. Sci.* **37**: 130–137.
- VOELKER, B. M., F. M. M. MORELL, AND B. SULZBERGER. 1997. Iron redox cycling in surface waters: Effects of humic substances and light. *Environ. Sci. Technol.* **31**: 1004–1011.
- , AND D. L. SEDLAK. 1995. Iron reduction by photoproducted superoxide in seawater. *Mar. Chem.* **50**: 93–102.
- VON SONNTAG, C., AND H.-P. SCHUCHMANN. 1997. Peroxyl radicals in aqueous solutions, p. 173–234. *In* Z. B. Alfassi [ed.], *Peroxyl radicals*. Wiley.
- WARD, J. V., K. TOCKNER, P. J. EDWARDS, J. KOLLMANN, G. BRETSCHKO, A. M. GURNELL, AND G. E. PETTS. 1999. A reference river system for the alps: The “fiume Tagliamento.” *Regul. Rivers Res. Mgmt.* **15**: 63–75.
- WETZEL, R. G. 1992. Gradient-dominated ecosystems: Sources and regulatory functions of dissolved organic matter in freshwater ecosystems. *Hydrobiologia* **229**: 181–198.
- , P. G. HATCHER, AND T. S. BIANCHI. 1995. Natural photolysis by ultraviolet irradiance of recalcitrant dissolved organic matter to simple substrates for rapid bacterial metabolism. *Limnol. Oceanogr.* **40**: 1369–1380.

Received: 22 October 2002

Accepted: 22 August 2003

Amended: 10 October 2003